MTI/ISS-IMAP/SLATS研究集会@情報通信研究機構 2015年9月2日

低高度衛星観測から期待される超高層大気研究の進展

藤原 均
成蹊大学 理工学部

概要

- 超高層大気の研究課題のいくつか
  特に、高度100-300 kmでの科学的(社会的)研究意義

- これまでの低高度衛星(< 300 km)による観測例

- 将来の衛星観測へ期待すること

- まとめ

熱圏の大気

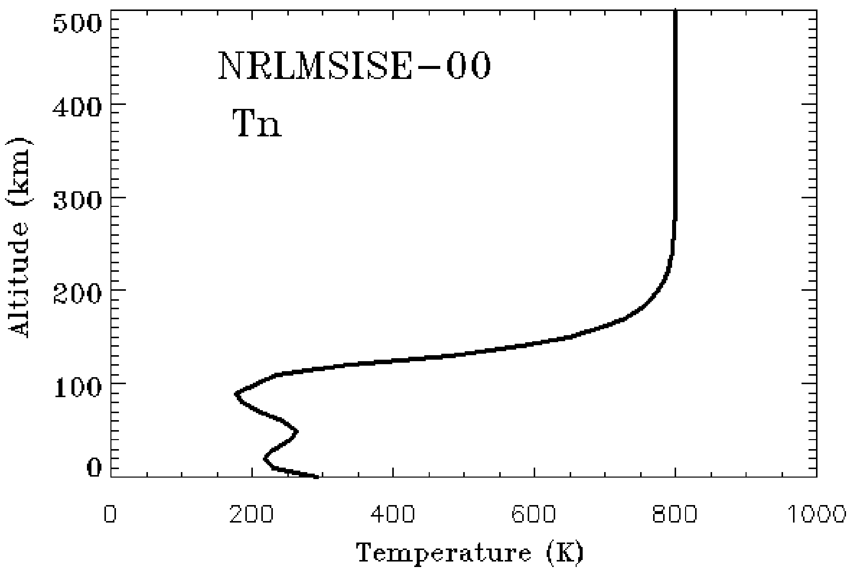
NRLMSISE-00
Tn
Altitude (km)
0
100
200
300
400
500
0
200
400
600
800
1000
Temperature (K)

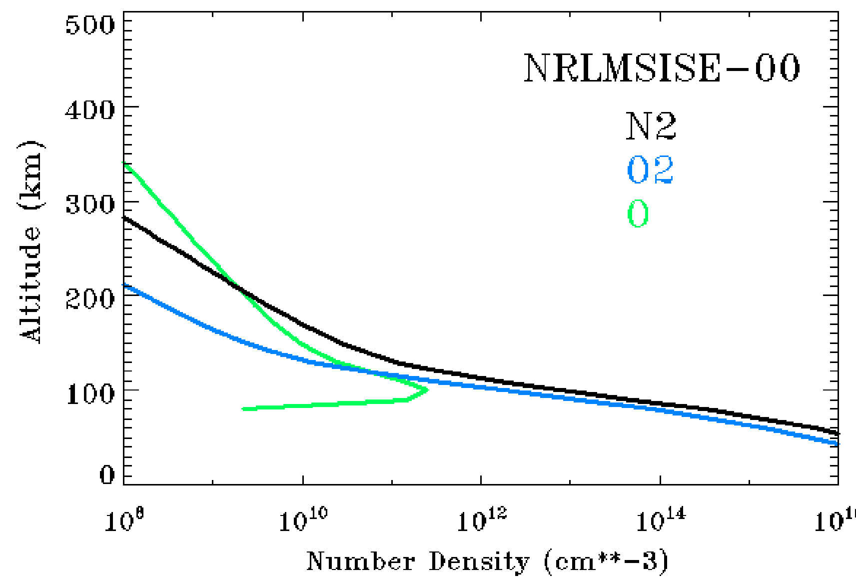
NRLMSISE-00
N2
02
0
Altitude (km)
0
100
200
300
400
500
10^{8}
10^{10}
10^{12}
10^{14}
10^{16}
Number Density (cm**-3)

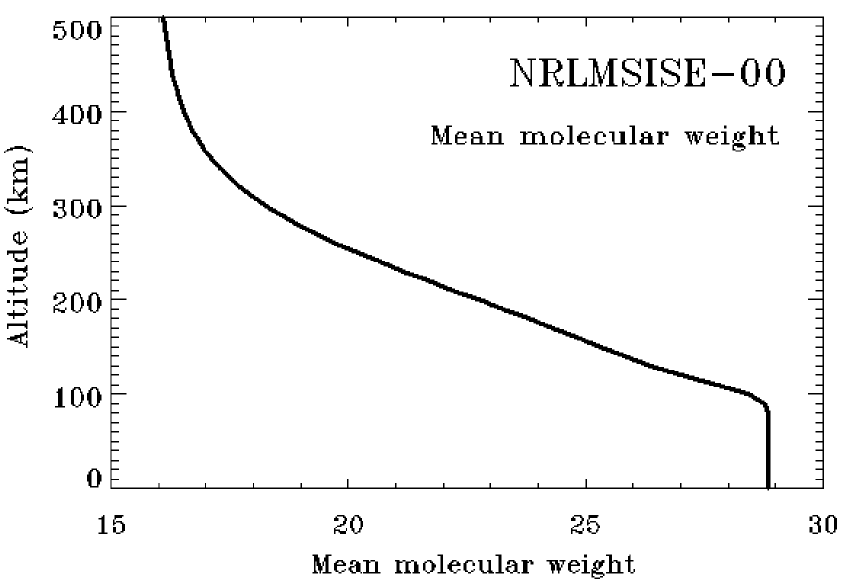
NRLMSISE-00
Mean molecular weight
Altitude (km)
0
100
200
300
400
500
15
20
25
30
Mean molecular weight

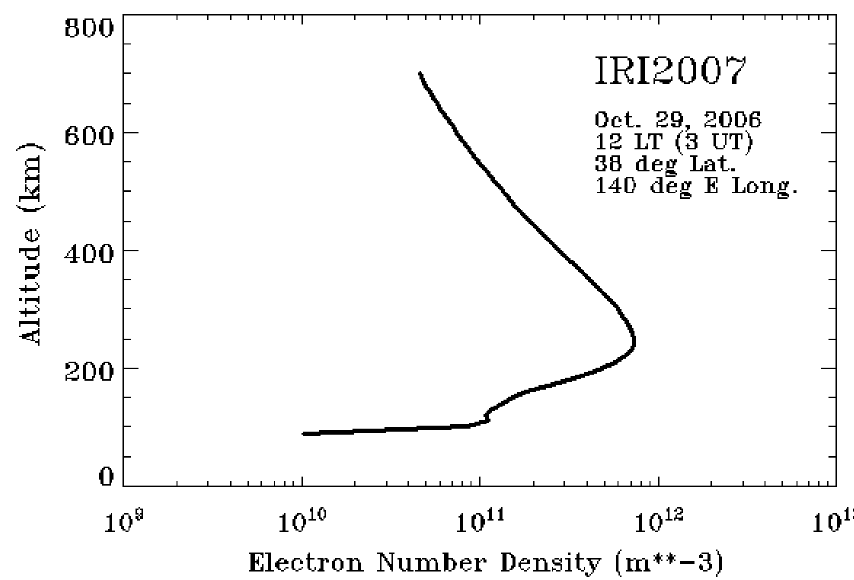
IRI2007
Oct. 29, 2006
12 LT (3 UT)
38 deg Lat.
140 deg E Long.
Altitude (km)
0
200
400
600
800
10^{9}
10^{10}
10^{11}
10^{12}
10^{13}
Electron Number Density (m**-3)

Examples of GCM simulation (Fujiwara et al., 2011)

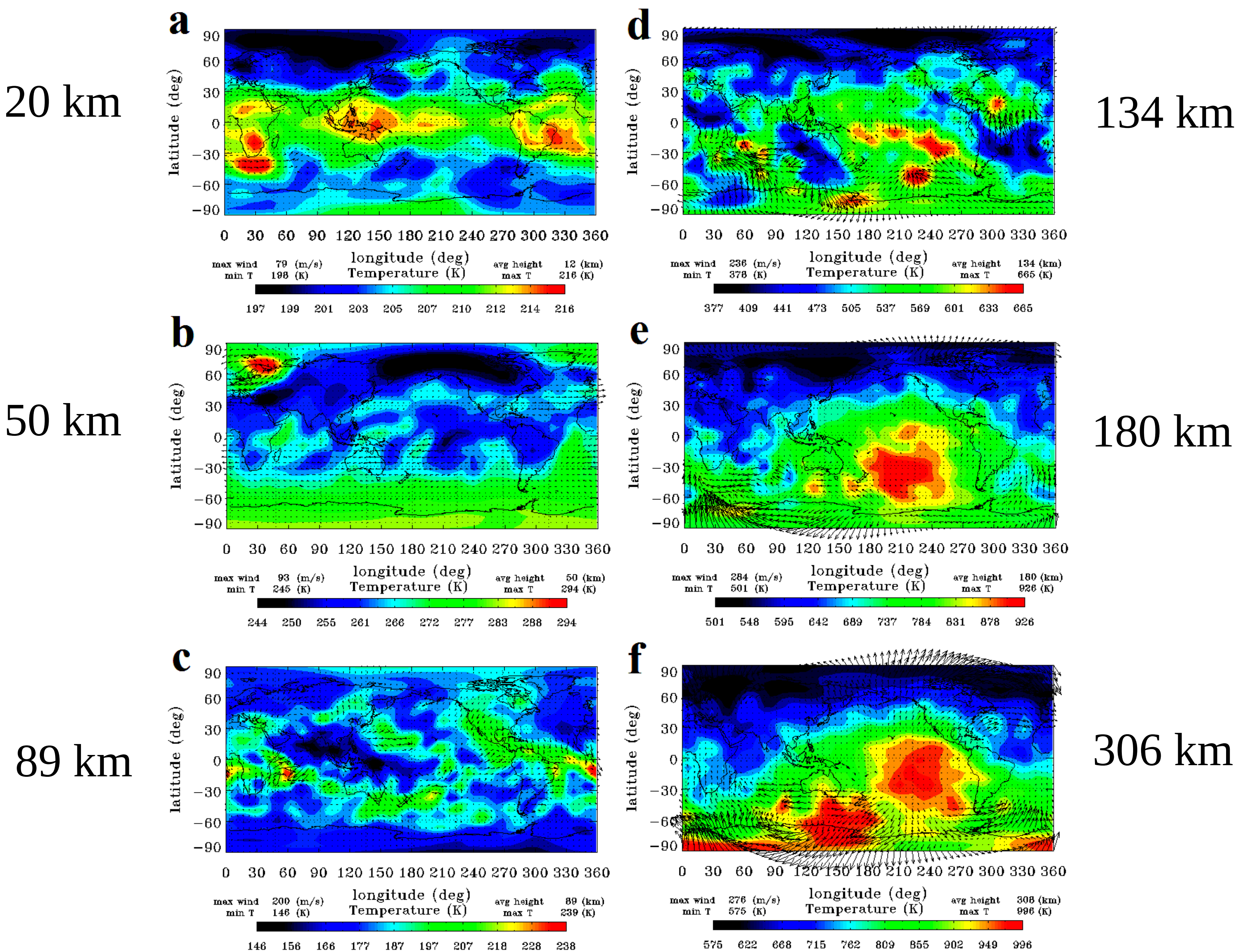

高度100～200 km付近では、温度、組成（平均分子量）、電子密度が高度とともに急激に変化する。

この高度範囲での、温度、質量密度、組成、風速･･･の高度分布の**観測例は極めて少ない**。

＊温度分布→エネルギー収支とコンシステントか？
寒冷化との関係は？
＊組成（特に赤外放射に関わる微量成分と酸素原子）は？
＊風速分布
→波の伝搬との関係は？
この領域での風の加速機構は十分にわかっているか？

熱圏大気質量密度減少の長期トレンド

Mass density trend due to greenhouse cooling

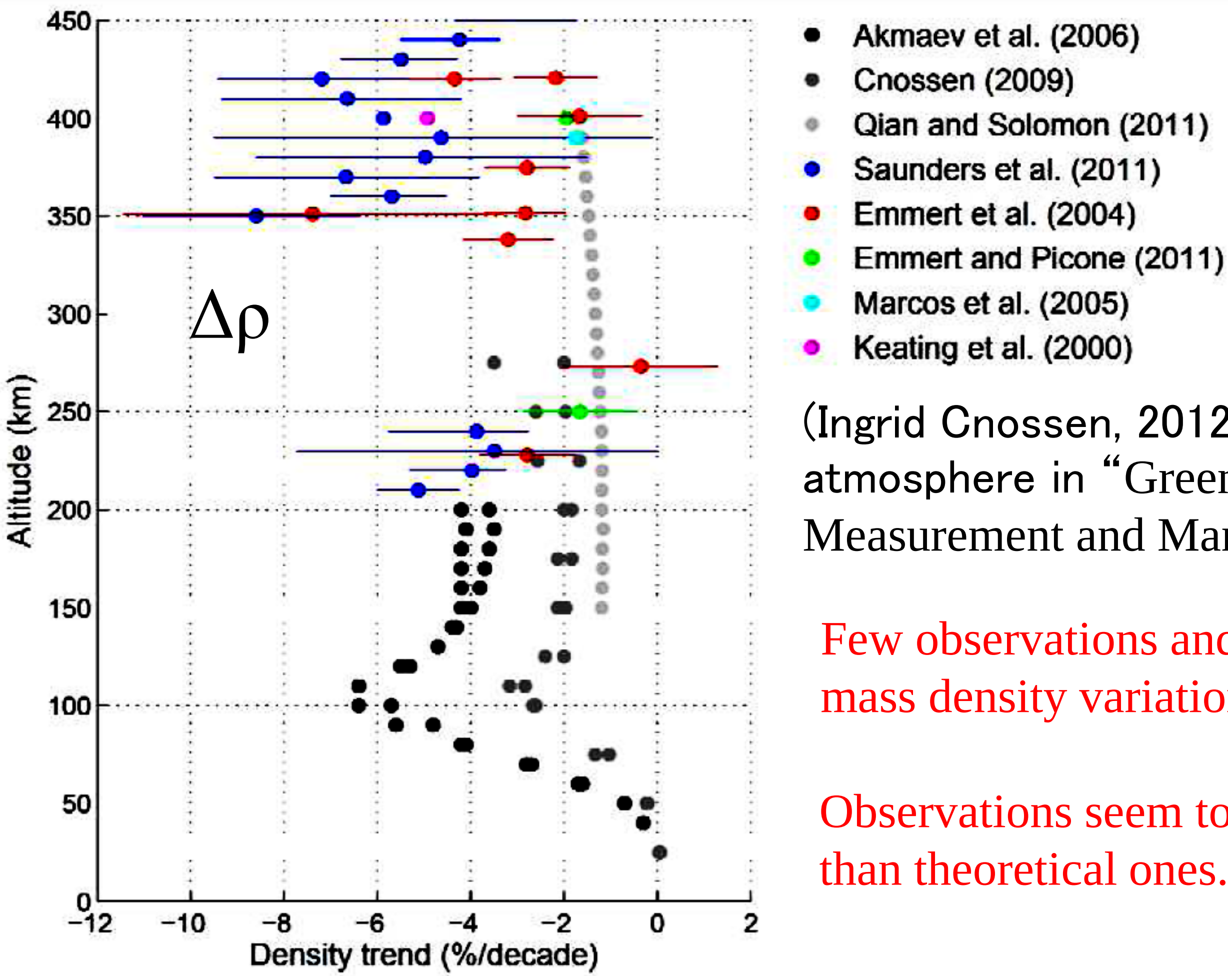

高度
~ 250-350 km
< 200 km
では、トレンドを議論できるデータがない！

(Ingrid Cnossen, 2012: Climate change in the upper atmosphere in "Greenhouse Gases - Emission, Measurement and Management", www.intechopen.com)

Few observations and many uncertainties for mass density variations.

Observations seem to show larger cooling than theoretical ones.

熱圏での赤外放射冷却

- CO$_2$ cooling at 15 µm (peaks ~ **120 km**)
- NO cooling at 5.3 µm (peaks ~ **150 km**))
- O(^{3}P) fine structure cooling at 63 µm (maximizes > 200 km)

（Burns et al. [2011, Chapman conference ppt]より）

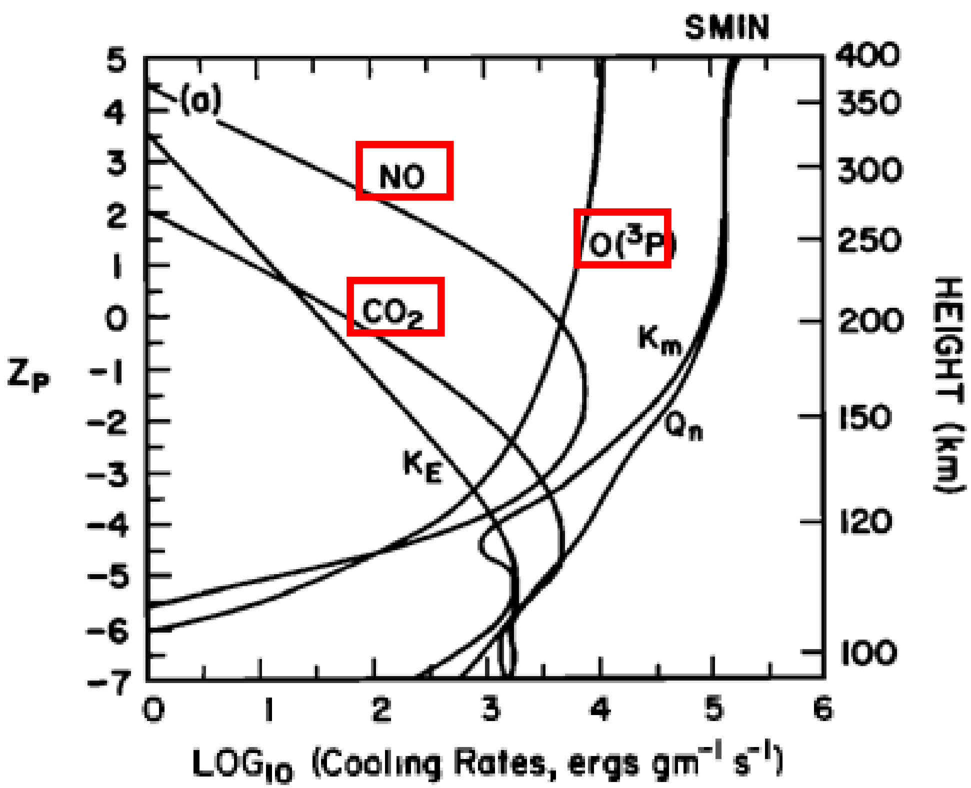

Global mean cooling rates in the thermosphere by NCAR 1D model

(Roble et al., JGR, 1987)

CO_2、NOからの全赤外放射量

Infrared radiation from the thermosphere to space

Mlynczak, M. G., L. A. Hunt, C. J. Mertens, B. Thomas Marshall, J. M. Russell III, T. Woods, R. Earl Thompson, and L. L. Gordley (2014), Influence of solar variability on the infrared radiative cooling of the thermosphere from 2002 to 2014, Geophys. Res. Lett., 41, 2508-2513, doi:10.1002/2014GL059556.

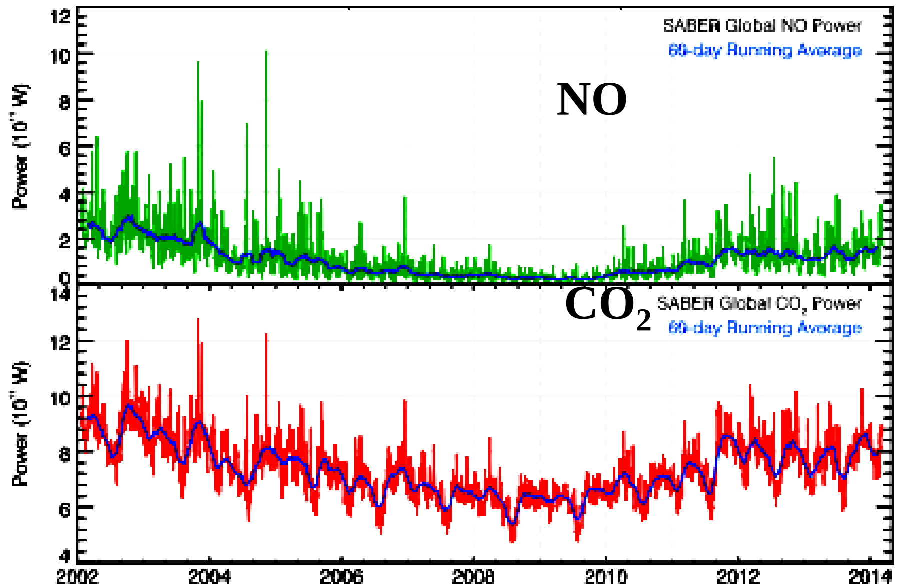

Figure 1. Time series of SABER daily global infrared power for (top) NO and (bottom) CO_2, from 22 January 2002 to 11 March 2014. The 60 day running mean is shown by the blue curve in both cases. Data from more than 4400 days of SABER observations are in each series.

Total Global CO_2 Cooling Power

$O+CO_2$ reaction coefficient

	Baseline Model $k_O=1.5x10^{-12}$	Mod #1 $k_O=6x10^{-12}$	Mod #2 EUV_{min} x 1.18 k_{zz} / 2 $k_O=6x10^{-12}$	Typical SABER annual average
Solar Min	330	420	510	700
Solar Max	510	590	650	900

Integrated global cooling rate in GW

Solomon et al. *TREND 2012 Workshop , 2012*

モデルでは赤外放射が過小評価のようである
寒冷化の進み具合(K/decade)は、モデルが過小評価といった先行研究と整合的

原因は？　→　100〜150 kmの高度範囲で、CO_2とOの両方がわからなければ決着はつかない

高度200 km付近での熱圏大気質量密度変動

レーダーによるプラズマ計測以外には、ロケット観測などがまれにあるだけでほとんど観測が行われていない。

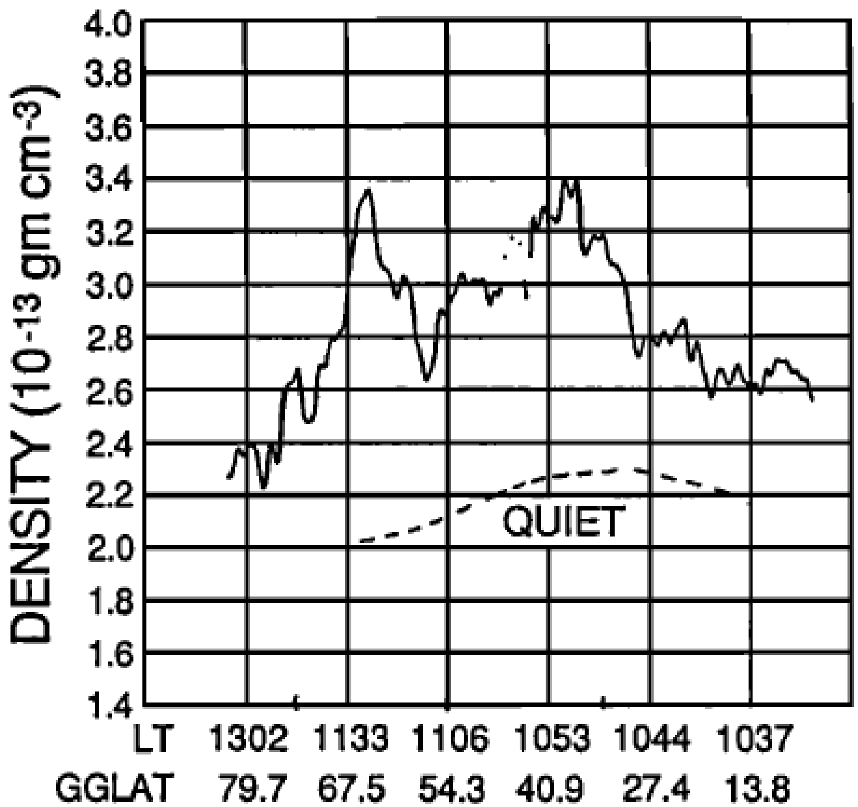

Figure 1. Comparison of measured density variations for active (solid curve) and quiet (dashed curve) conditions at 200 km as a function of geographic latitude for a polar orbiting satellite in the 1040-2240 LT plane.

Crowley et al. [JGR, 1996]
高度200kmでの中性大気密度変化.
地磁気静穏時と擾乱時(Kp~5)の比較.

San Marco satellite

Crowleyらは、観測された密度分布をcellular structure (又はdensity cell)と呼び、極域に現れる２～４の高(低)密度領域を衛星が通過したことによると考えた。

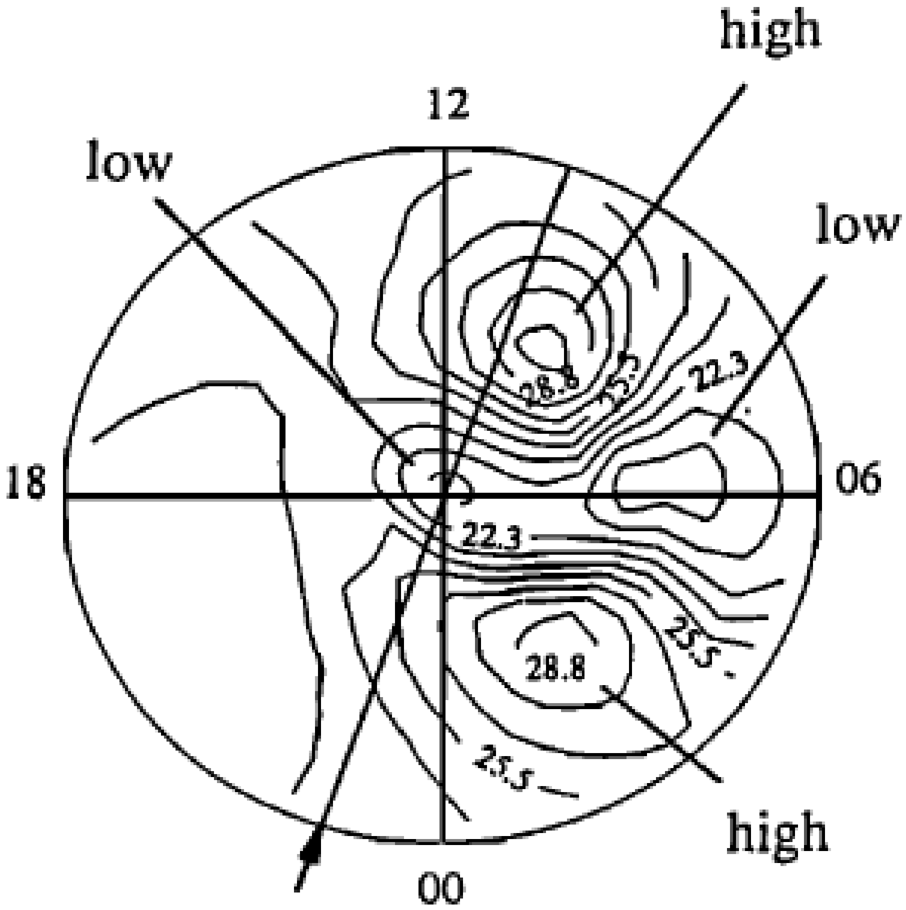

NCAR-TIGCMによるシミュレーション.
高度200 km、
Cross polar cap potential drop = 90 kV

これまでの主な超高層大気観測ミッションの例

AEROS, Alouette, Atmospheric Explorer (AE)
Dynamics Explorer (DE)
Upper Atmosphere Research Satellite (UARS)
Thermosphere Ionosphere Mesosphere Energetics and Dynamics (TIMED)
Cosmic/FORMOSAT, C/NOFS
Aeronomy of Ice in the Mesosphere (AIM)
Odin satellite, SCISAT-1(ACE-FTS)

NOAA satellites
Defense Meteorological Satellite Program (DMSP)
GPS → Total electron content
CHAMP, GRACE, SWARM, GOCE

ISS-IMAP

たいよう(SRATS)、ひのとり、おおぞら、あけぼの、れいめい、（Geotail） ・・・

Year	Experiment	Data	Lifetime	Agency
1981	DE-2	Composition	18 Mos.	NASA
1982	SETA-2	Density	8 Mos.	AFRL
1983	SETA-3	Density	8 Mos.	AFRL
1985	S85-1	Density	3 Mos.	AFRL
1988	San Marco	Density	8 Mos.	NASA
1999	LORAAS	Composition	3 Yrs.	NRL
2000	CHAMP	Density	5+ Yrs.	GFZ Potsdam
2001	TIMED GUVI	Composition	4+ Yrs.	NASA/APL/Aerospace
2002	GRACE	Density	3+ Yrs.	CSR, Texas
2003	SSULI/SSUSI	Composition	3+ Yrs.	DMSP/APL/NRL
2003	ORBITAL DRAG	Density	30+ Yrs.	AFRL/AFSPC/NRL

Figure 2 Satellite density measurements before and after the year 2000

(Marcos, AIAA 2006)

Cross-track wind from the accelerometer onboard the **SETA satellite**

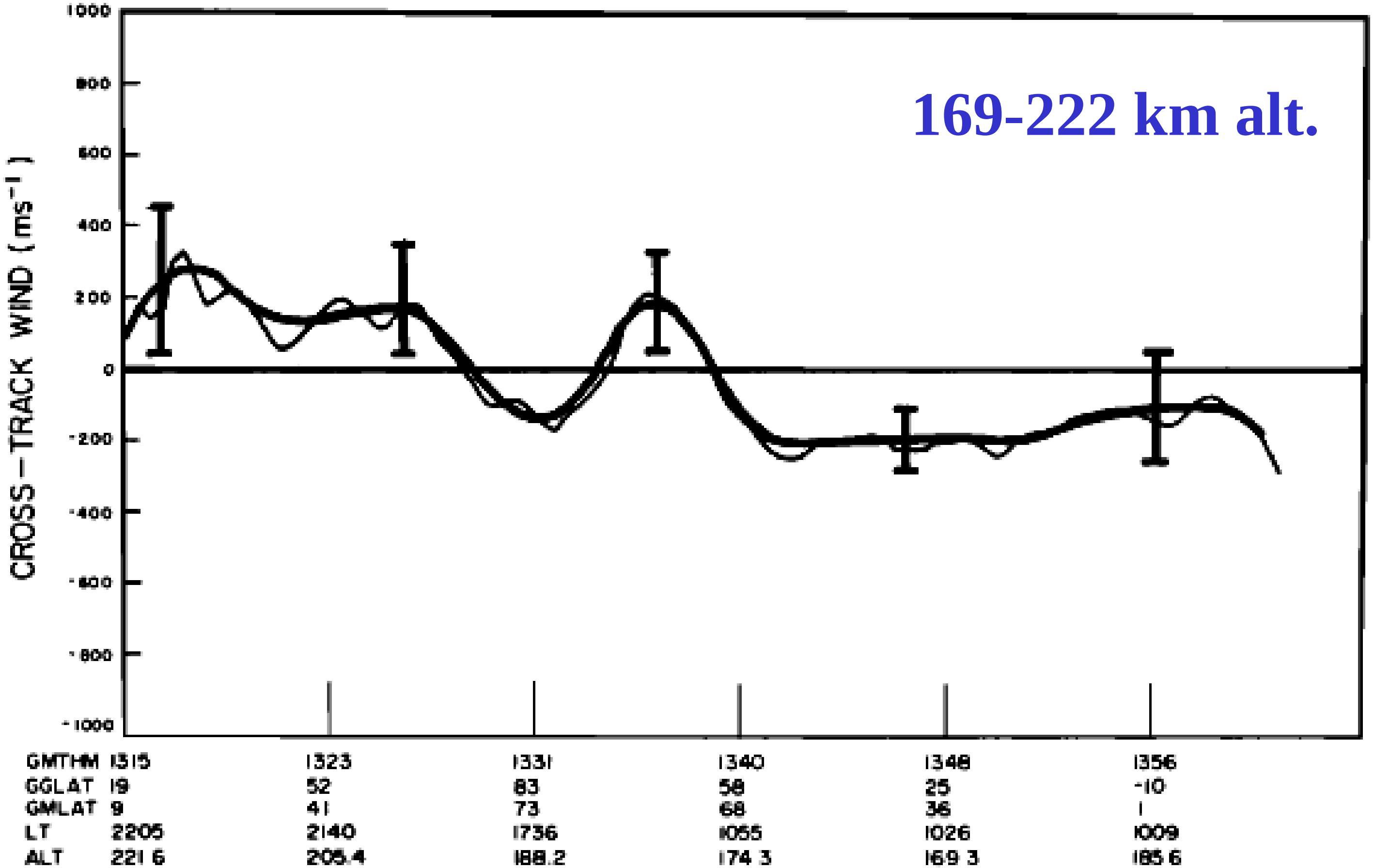

Fig. 5. Cross-axis winds corresponding to the data in Figure 4 plotted verus universal time, geographical latitude, geomagnetic latitude, local time, and altitude. Unsmoothed (light line) and smoothed (heavy line) data are shown. Error bars on the smoothed data primarily reflect uncertainties due to vehicle vibration noise (see section 2).

(Marcos and Forbes, JGR1985)

200 km alt.
July 20-23, 1983

Day Night

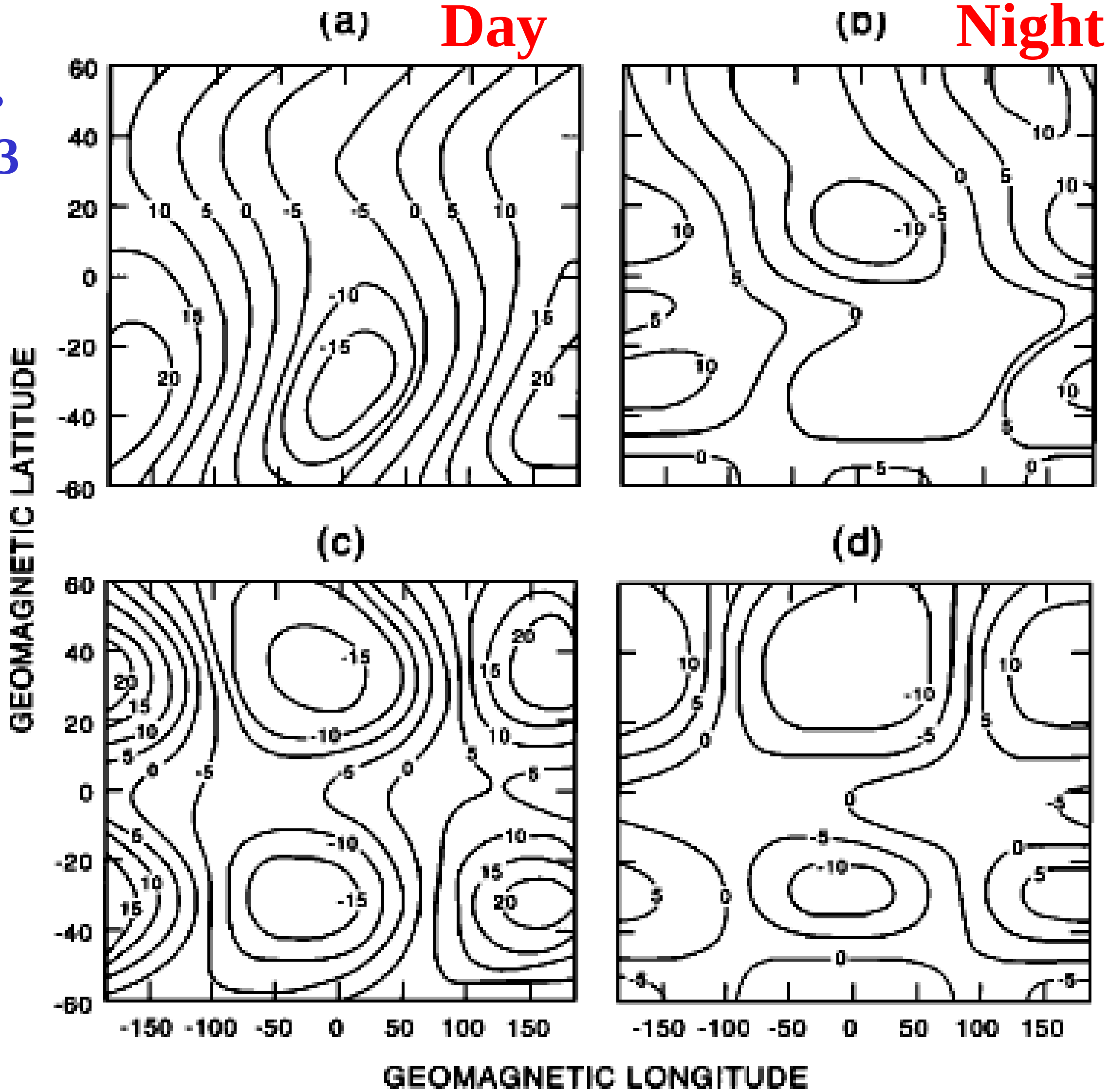

SETA

MSIS

Figure 4. Longitude/UT effect as revealed in (a) and (b) SETA and (c) and (d) MSISE-90 total mass densities (percent variation about quiet-time densities, as in Figure 3) at 200 km during July 20–23, 1983. (left) Daytime is ~1030 LT. (right) Nighttime is ~2230 LT. The scales correspond to −15% to +20% (daytime) and −10% to +10% (nighttime).

(Forbes et al., JGR1999)

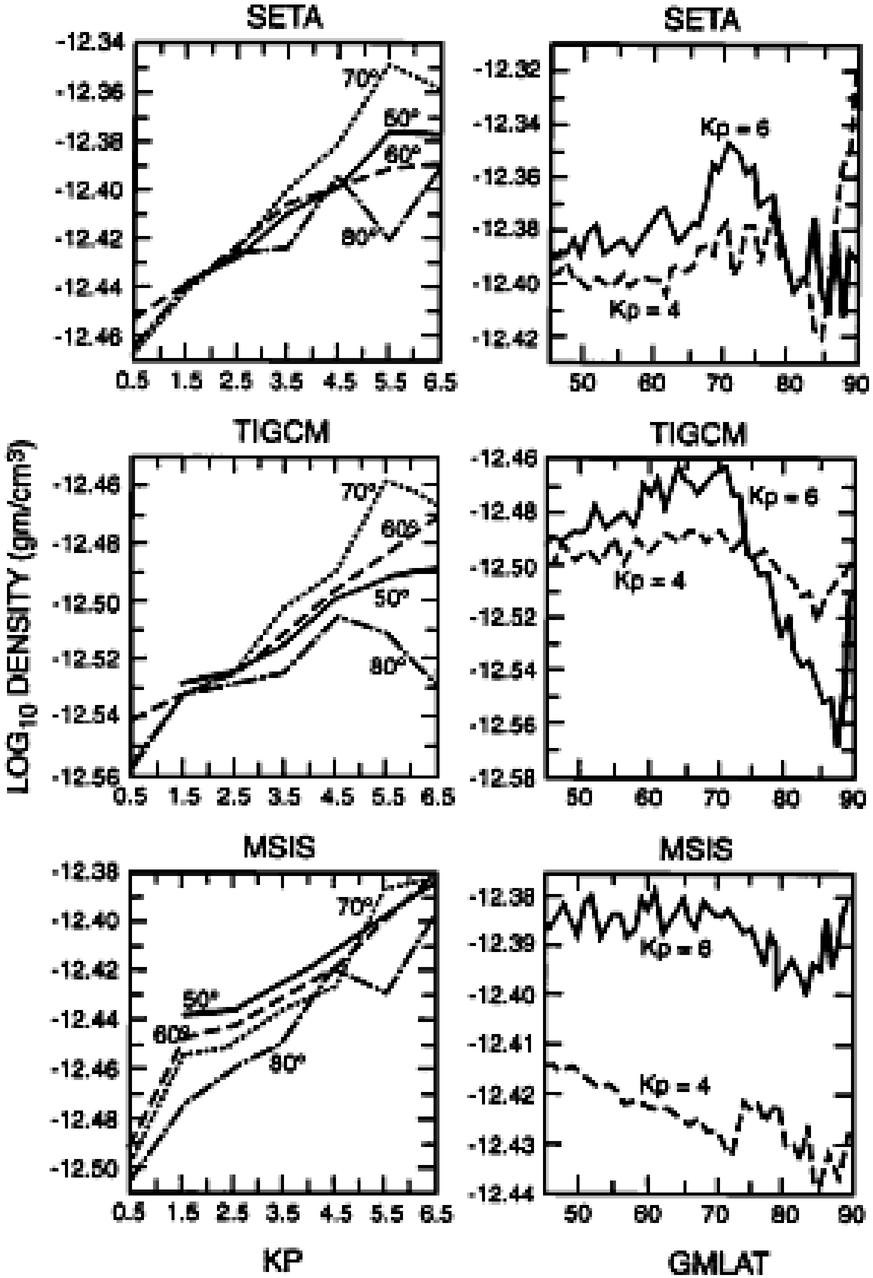

Fig. 6. Daytime densities at 200 km as a result of one-unit K_p binning and 10° latitude binning over the 20-day observational period. (Top) SETA densities (normalized to 200 km) (left) versus K_p at various geomagnetic latitudes and (right) versus geomagnetic latitude for K_p = 4.0 and 6.0. (Middle) Same as top figures, except for the TIGCM at 200 km. (Bottom) Same as above, except for the MSISE90 model at 200 km.

高度約200 kmでのρの緯度変化

(Forbes et al., JGR1993)

GEOPHYSICAL RESEARCH LETTERS, VOL. 27, NO. 9, PAGES 1387-1390, MAY 1, 2000

1994, 1997にスペースシャトルから放出

A global measurement of lower thermosphere atomic oxygen densities

K. U. Grossmann, M. Kaufmann, and E. Gerstner
Department of Physics, University of Wuppertal, Wuppertal, Germany

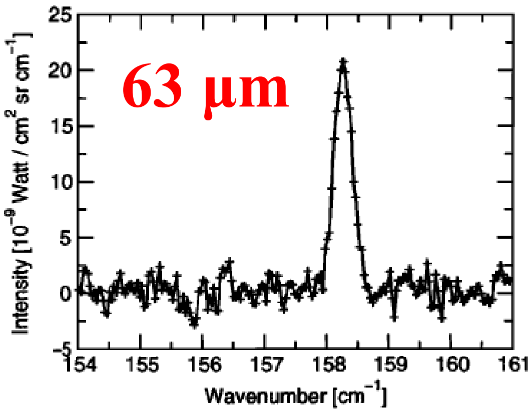

Figure 1. Single spectrum of the O(^{3}P) emission line at 63 µm recorded by CRISTA-2 at an altitude of 151 km.

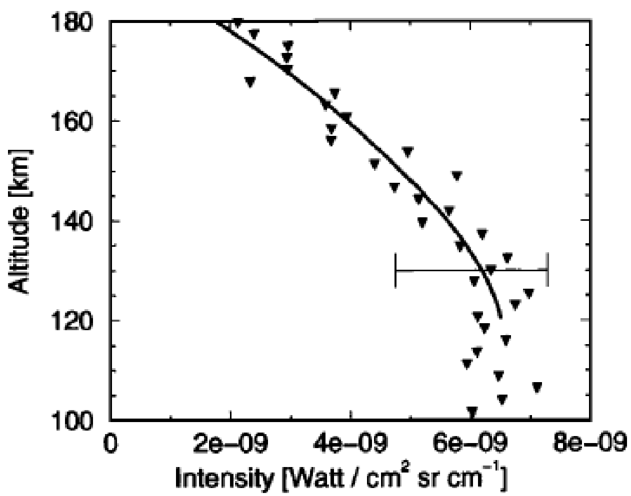

Figure 2. Line integrated limb radiance profile (CRISTA-2, one altitude scan). For details see text.

140 km

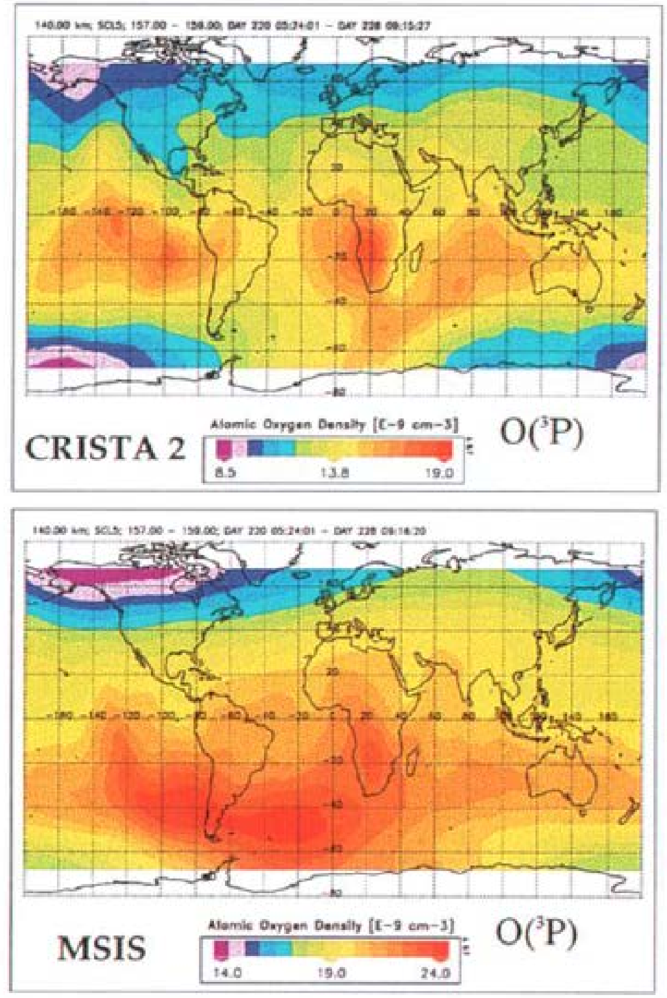

Plate 1. Atomic oxygen concentrations at 140 km measured by CRISTA-2 August 13 – 15, 1997 (upper panel). The color scale is 8.5 – 19.0 · 10^9 cm^{-3} in increments of 0.7 · 10^9 cm^{-3}. MSIS model atomic oxygen concentrations (lower panel) calculated for the conditions of the experimental data. The color scale here is 14.0 – 24.0 · 10^9 cm^{-3} in increments of 0.7 · 10^9 cm^{-3}.

下部熱圏での酸素原子密度推定例

- 63μm放射、balloon platform at 37 km

JOURNAL OF GEOPHYSICAL RESEARCH, VOL. 92, NO. D4, PAGES 4325–4336, APRIL 20, 1987

Atomic Oxygen in the Lower Thermosphere

Florence J. Lin, Kelly V. Chance, and Wesley A. Traub

Harvard-Smithsonian Center for Astrophysics, Cambridge, Massachusetts

We measured in thermal emission the 63-μm line due to thermospheric atomic oxygen $O(^3P)$, using a far-infrared spectrometer on a balloon platform at 37 km altitude over Palestine, Texas (32°N), on June 20, 1983. From measurements of the equivalent width of this line at two elevation angles, we find a weak angular dependence: the equivalent width increases by a factor of 1.5 ± 0.3 as the angle decreases from $+30°$ to $+1°$. Since the optical depth of the $O(^3P)$ line is large, we cannot directly convert the measured line intensity to a column abundance. Instead, we interpret the measurements in terms of radiative transfer through a 16-layer atmosphere extending to 200 km. We use a model atmosphere for summer at 30°N, with an exospheric temperature of 1300 K, including (1) an assumed daytime atomic oxygen abundance profile constructed from recent chemical and dynamical models and (2) a water vapor abundance profile constructed from recent experimental and model results. For this assumed $O(^3P)$ vertical profile shape we determine from our spectra at two elevation angles a multiplicative scaling factor of 0.8, with an altitude-dependent uncertainty. In the best-determined layer the uncertainty in the multiplier is ± 0.2 at 119 km. The model-dependent peak atomic oxygen density is $3.6\ (\pm 1.9) \times 10^{11}$ cm^{-3} at an altitude of about 101 km.

http://www.nasa.gov/mission_pages/aim/overview/index.html

A NASA spacecraft scheduled for launch in 2006 should provide some answers. The *Aeronomy of Ice in the Mesosphere* satellite, or AIM for short, will orbit Earth at an altitude of 550 km. Although it's a small satellite, says Thomas, there are many sensors on board. AIM will take wide angle photos of NLCs, measure their temperatures and chemical abundances, monitor dusty aerosols, and count meteoroids raining down on Earth. "For the first time we'll be able to monitor all the crucial factors at once."




2007 May 20

高度100～200 km付近での研究課題例のまとめ

＊CO_2、Oの分布
＊質量密度の変動(density cell)
＊熱圏高速風？
＊NLC、大気光の微細構造→大気重力波の微細構造

超低高度衛星から（間近から）のリモートセンシング

社会的な意義

中間圏・熱圏の寒冷化→対流圏の温暖化 のモニタリング

宇宙への玄関口の環境を知る→将来の高度な宇宙機の運用のための基礎情報

超低高度からのリモートセンシング技術・データ利用の可能性

Summary

低高度 (< 200 km)での密度計測の例はそれなりにはある。また、経験モデル（MSIS）との比較もされている。密度の局所構造（赤道非対称性）などは十分に説明はされていない？
時系列での変動についての議論はない？（少ない？）

高高度では、CHAMP、GRACE以降、様々な例が示された。特に、地磁気擾乱時の密度構造のClimatologyがそれら以前とは比べ物にならない。地磁気擾乱時の予測への準備が進みつつある？（Guo et al., 2010）。
ただし、静穏時が完全に理解されているかは疑問。例えば、Oberheide et al. (2011)では外気圏での半日・一日潮汐の振幅とその場加熱によるものとを議論。太陽活動依存性 (Bruinsma et al., 2010) や、CO_2増加の影響の議論(Akmaev, 2012) は続いている。

超高層大気の寒冷化との関係で、高度100-200 kmに赤外放射のピークをもつCO_2と、CO_2との反応が重要であるOの時空間変動の理解が不可欠（赤外放射量、温度・密度の減少トレンドのモデルと観測との不一致の原因究明のため）。

また、超低高度からのリモートセンシングにより、大気光や夜光雲の微細構造の可視化→重力波砕波の可視化が有効かもしれない。

高度100-200 kmは、衛星運用・利用の面だけでなく、大気科学のフロンティア領域でもある。

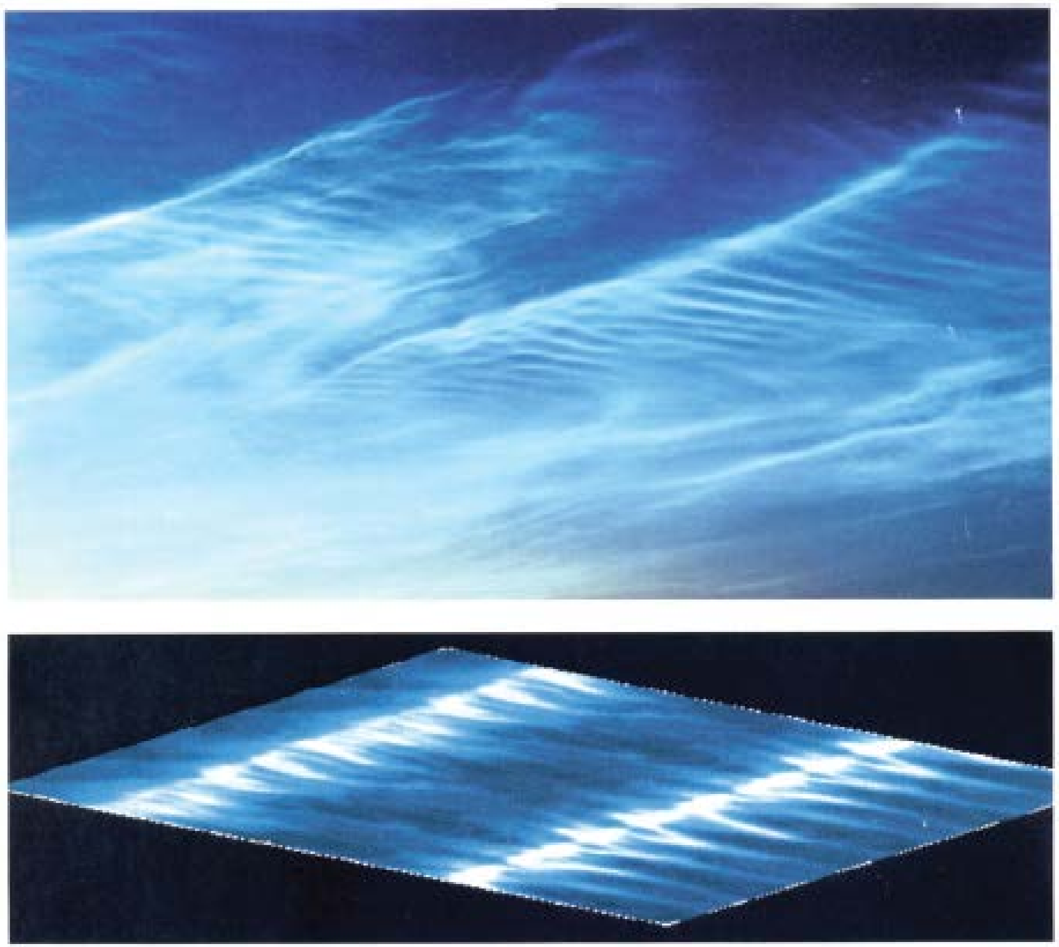

Figure 16. (top) Observed and (bottom) simulated gravity wave and instability structures in NLC. Photo was taken at Turku, Finland, on 21–22 July 1989, courtesy of Pekka Parvianien. Streamwise-aligned instability structures are believed to have accounted for the smaller-scale bright bands oriented approximately normal to the gravity wave phase fronts in the upper image. After *Fritts et al.* [1993b].

? ?

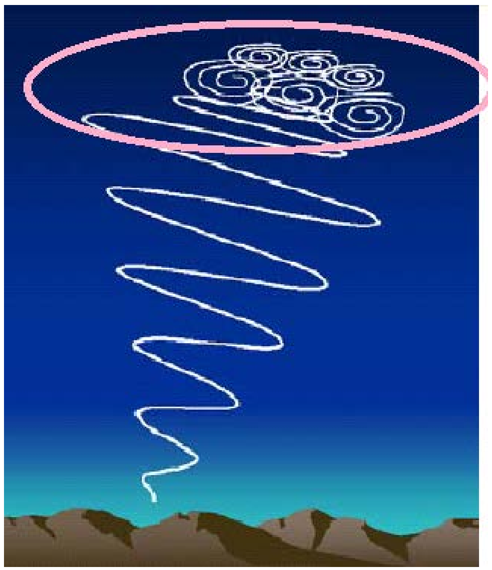

Fritts and Alexander
(Rev. Geophys., 2003)

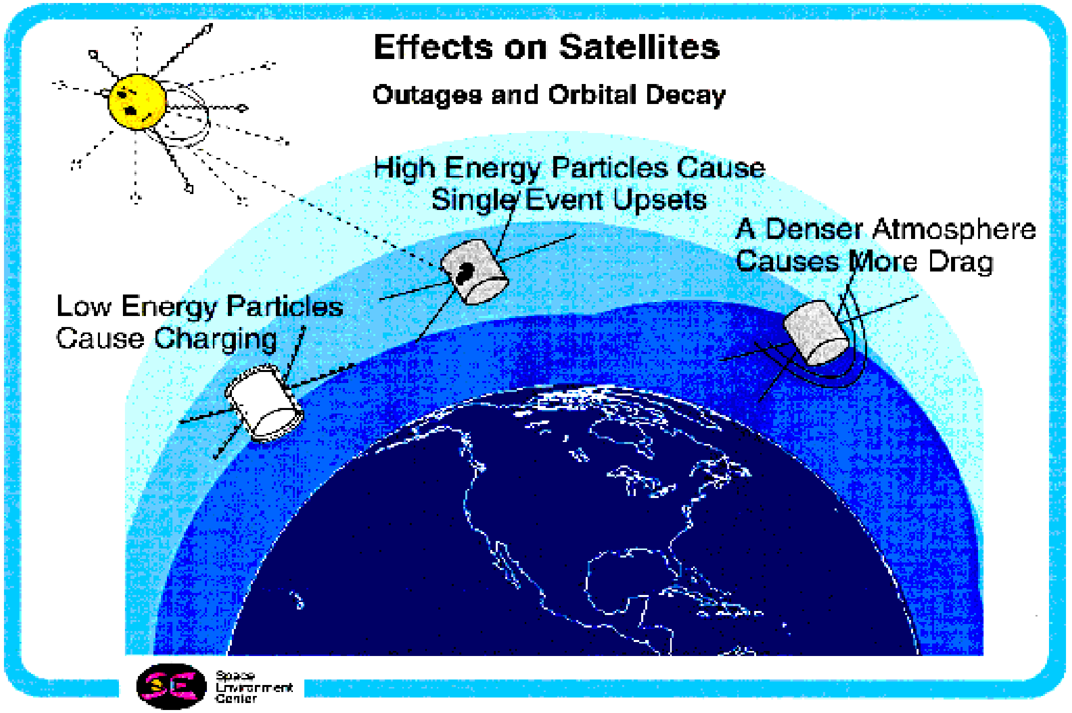

$$\frac{dr}{dt} = -\frac{\rho V C_D A_r r}{m} \Longleftrightarrow \rho = -\frac{m}{V C_D A_r r}\frac{dr}{dt}$$

キーパラメータ: A/m

Relative effects of CO_2 cooling

Venus : very effective
Mars : effective
Earth : not so effective

e.g., Bougher and Roble (JGR, 1991)

O/CO_2 is one of key parameters for energetics in the terrestrial planets, Venus and Mars.

In case of the Earth, O/N_2 is important.